Block-Filtered OFDM: a novel waveform for future wireless technologies

David DEMMER*†, Robin GERZAGUET*, Jean-Baptiste DORÉ*, Didier LE RUYET† and Dimitri KTÉNAS*
*CEA-Leti, Minatec Campus, Grenoble, France
{david.demmer, robin.gerzaguet, jean-baptiste.dore, dimitri.ktenas}@cea.fr
†Conservatoire National des Arts et Métiers, 292 Rue Saint-Martin, 75003 Paris, France
{didier.le_ruyet}@cnam.fr

***Abstract*—The forthcoming fifth generation of mobile technology (5G) will be designed to satisfy the demands of 2020 and beyond. 5G does not just promise a huge increase in terms of data rates and capacity but it also targets new kind of use cases like Internet of Things or vehicular communications. The currently deployed 4G technology does not provide enough network capabilities to support this wide diversity of applications which has motivated the research on alternative waveforms. In this article, a new promising modulation scheme is introduced: Block-Filtered OFDM (BF-OFDM). The proposed waveform demonstrates an excellent frequency localization and can straightforwardly be integrated with the OFDM know-how and LTE principles. Besides, the proposed waveform relies on a receiver similar to the one used in CP-OFDM. BF-OFDM systems are also scalable, which is an interesting feature in order to steer the network capabilities on demand.**

I. Introduction

Accessing the internet on mobile has become fundamental for doing business and for personal use. It generates an ever-increasing demand in mobile data traffic which is considerably induced by broadband devices but also by the diverse emerging new use cases like the Internet of Things (IoT), tactile internet or ultra-reliable Machine-Type Communications (MTC) [1][2]. However, the currently deployed LTE-Advanced (LTE-A) network cannot provide enough network capabilities to support the expecting traffic demand and incremental evolution alone is not likely to be sufficient neither. Therefore, discussions to develop a mobile network compliant with our needs have started for a deployment scheduled for 2020 [2].

Significantly wider contiguous spectrum bandwidths are predicted for 5G: from hundreds MHz to a few GHz [3]. Spectrum above 6GHz is thus considered to satisfy the huge demand of wide contiguous bandwidth. Nevertheless, sub-6GHz bands provide desired propagation characteristics for wide range applications. That is why 5G should still use these bands but efficiently in order to maximise the bandwidth use and improve coexistence with non-mobile systems. For such applications, dynamic spectrum sharing is considered [1][3]. Cyclic Prefix Orthogonal Frequency Division Multiplexing (CP-OFDM) has prevailed in many wireless standards including LTE thanks to its high resilience against frequency selective channels and its straightforward hardware implementation by means of (Inverse) Fast Fourier Transform ((I)-FFT). However, it suffers from a poor spectral localization due to its rectangular pulse shape and thus cannot be adapted to narrowband spectrum availability [1]. Another drawback of the legacy CP-OFDM is its lack of flexibility which proves to be inconsistent with the heterogeneity of the future network. These two latter aspects makes CP-OFDM poorly appealing for 5G and have motivated the study of alternative waveforms. Current research has mainly concentrated on two families of waveforms: sub-carrier (with Filter Bank Multi-Carrier -FBMC-) and suband filtering (with Universal Filtered Multi-Carrier -UFMC-).

UFMC has been introduced by Alcatel-Lucent [4]. A filtering is applied to a block of consecutive subcarriers. It provides low out-of-band (OOB) emissions and outperforms CP-OFDM in a few cases (e.g asynchronous transmissions [5]). However, this modulation scheme suffers from Inter-Symbol Interference (ISI) induced by multipath channels. Consequently, the robustness against frequency selective is reduced w.r.t. CP-OFDM. Besides, the implementation of the transmitter/receiver requires a high complexity that can eventually be reduced at the price of a slight performance decrease [6].Fast Convolutions (FC) have also been proposed to efficiently filter subbands of OFDM signals [7]. With a slight complexity increase, this scheme provides high rejection of interference leakage between subbands and flexibility. At the reception, the incoming signal is processed by subband as well.

On the other hand, the concept of filter bank was introduced in the mid-60s [8]. FBMC relies on a subcarrier-wise filtering. The prototype filter defines the localization of the signal in both time and frequency. Indeed, the key aspect of FBMC is to relax the orthogonality condition in order to improve its spectral confinement according to the Balian Low Theorem [9][10]. In order to come up with the loss of the complex orthogonality, Offset-Quadrature Amplitude Modulations (OQAM) are commonly used so as to only depend on the real orthogonality. FBMC/OQAM achieves the best spectral localization and has a particular interest in non-synchronous access among the aforementioned waveforms. However, the adaptation to Multiple Input Multiple Output (MIMO) techniques and channel estimation are not straightforward due to the inherent interference generated by the loss of the complex orthogonality [11]. Some precoded versions of FBMC/OQAM have been proposed in order to restore the complex orthogonality of the modulation scheme [12][13]. Both proposed solutions rely on a complex receiver that performs the decoding process. The waveform proposed in [12], FFT-FBMC, is *in fine* highly similar to the Resource-Block Filtered-OFDM scheme proposed in [14] but longer filter impulse response is considered for FFT-FBMC.

Besides, according to the agreement of 3GPP RAN1-86 meeting held in August 2016, new waveforms for the phase 1 of 5G (New Radio Work Item) should be specification transparent, i.e. the receiver does not need to know the filtering/windowing used at the transmitter. The aforementioned waveforms perform a matched filtering in reception and thus are not compliant with the latter specification.

In this paper, a novel modulation scheme is introduced: Block-Filtered OFDM (BF-OFDM). It is an improved version of FFT-FBMC [12] in the sense that the receiver can be reduced to a simple FFT and is therefore specification transparent. The proposed waveform provides a good spec-

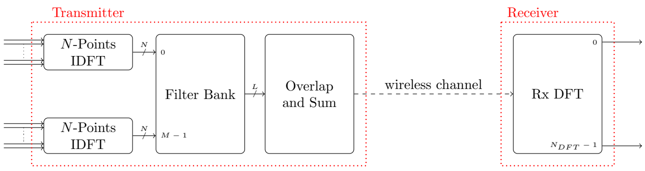

Figure 1. Considered Starting Architecture

tral localization with enhanced side lobes rejection while providing equivalent performance against frequency selective channels compared to CP-OFDM and satisfies the complex quasi-orthogonality (very low level of intrinsic interference). Moreover, it excels in multi-user scenarios and is fully flexible [15]. Hence, BF-OFDM is a promising candidate to be considered for future wireless technologies.

The aim of this paper is to give an overview of the waveform and to derive the working conditions. In Section II, the BF-OFDM concept is detailed. Key Performance Indicators (KPIs) are assessed in Section III. Finally, concluding remarks and study perspectives appear in Section IV.

II. BF-OFDM PRINCIPLES

A. General principle and motivations

Multi-carrier modulations have proved to be an efficient transmission scheme over selective channels. Besides, filtering stage provides high OOB rejections. In addition to that basic unit of resource allocation is a group of carriers (e.g. 180kHz resource block with twelve carriers for LTE) which encourages filtering at the sub-band level. For these reasons, a transmitter composed of a filter bank (with Inverse Discrete Fourier Transform (IDFT) and a PolyPhase Network (PPN) stage) is considered. In order to cancel the intrinsic interference induced by the filter bank a IDFT-based precoding stage is added as studied in [16]. The overlap and sum stage at the output of the filter bank aims at improving the spectral efficiency. The transmitter scheme is depicted in Fig.1. Our system will be designed so as to be able to demodulate the transmitted signal with only a Discrete-Fourier Transform (DFT) at the receiver side.

B. Receiver parametrization

The goal of this section is to characterize the Rx DFT (in both placement and size) to be able to properly recover the transmitted symbols.

Input symbols are spread over N transmitted frames by the joint action of the IDFTs and the filter bank. Frames are transmitted every Δ samples. Thus, two consecutive symbols are separated by N overlapped frames as illustrated in Fig.2 (a). In this figure, the useful symbol is depicted with the N white overlapped frames whereas the frames belonging to the two adjacent symbols are in blue.

If L denotes the length of one filtered frame (assuming that L is a multiple of Δ), the length of a symbol is $L+\Delta(N-1)$ samples.

It is assumed that the receiver is perfectly synchronized, *i.e.* it knows the starting position of the symbols.

A first approach would be to apply a Rx DFT size whose length corresponds to the size of the symbol and synchronized with its beginning as illustrated in Fig.2 (a). With such a DFT input window, the useful frame is entirely captured (all the N white frames). However, some interferences from the two adjacent symbols in time are captured as well (blue frames). A solution to cope with the ISI is to insert a Guard Interval (GI) which length corresponds to the number of frames belonging to the adjacent symbol that overlap with the useful one (as the blue frames become part of GI and are full of zeros).

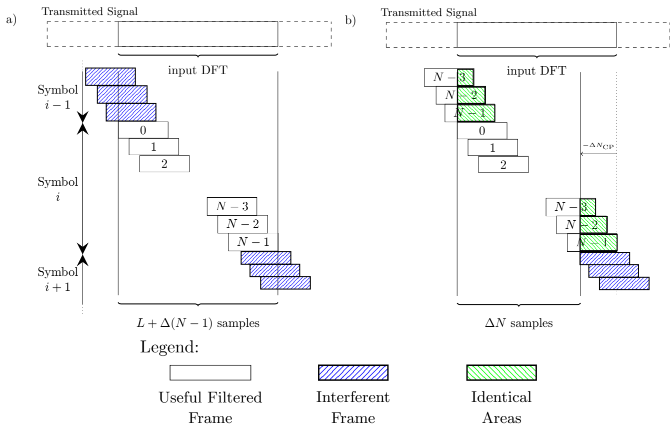

Figure 2. Inserting a CP both cancels ISI and reduce the receiver DFT size

It is worth noticing that it is possible to decrease the size of the DFT (i.e. receiver complexity) by using a Cyclic Prefix (CP) instead of the GI as shown in Fig.2 (b) (where N_{CP} denotes the length of the CP). Indeed, as the CP repeats the tail of the symbol, it is possible to reduce the size of the DFT by ΔN_{CP} samples (keeping the same starting point) and thus avoiding ISI coming from the CP of the following symbol (blue frames).

It is worth noticing that the insertion of a CP is a necessary condition to ensure proper recovering of the symbol (which is a difference w.r.t. CP-OFDM). Nevertheless, as the CP is spread in time, it also absorbs interference signal energy dispersed by the channel (within the limits of its size) as in CP-OFDM.

From the latest comments, it is possible to derive the conditions to avoid ISI with a reduced-size DFT in reception:

$$N_{CP} \geq \frac{L}{\Delta} - 1 \tag{1}$$

The corresponding Rx reduced-DFT size is ΔN (assuming that N_{CP} takes the minimum value satisfying (1)).

If a filter bank similar to the one used for FBMC/OQAM is considered [10], $L = KM$ where K is the overlapping factor of the filter (typically equal to 4) and Δ is $\frac{M}{2}$ [10]. The condition (1) applied to such a configuration leads to:

$$N_{CP} \geq 2K - 1 \tag{2}$$

The reduced-DFT size is thus $\frac{MN}{2}$. This configuration will be considered for the rest of the paper.

C. Intra-Carrier Orthogonality

The section aims at deriving the conditions that must be satisfied by the input signals in order to ensure its proper recovering at the reception.

In this section, a transmission over an unique precoding IDFT r_0 with an unique active sub-carrier q is considered. The insertion of a CP compliant with (2) between the precoding and filter bank stages is performed. The signal at the input of the filter bank is $(N+N_{\mathrm{CP}})$-sample long and can be expressed as follows:
$\forall t \in [0, N+N_{CP}-1]$

$$s(r,t) = \begin{cases} s_{r_0} e^{j\frac{2\pi}{N}q(t-N_{CP})} \text{ for } r = r_0 \text{ with } q \in \mathbb{Z} \\ 0 \text{ otherwise} \end{cases} \quad (3)$$

where s_{r_0} is the complex symbol feeding the precoding IDFT.

Under the assumption of an ideal channel and a noiseless transmission and by using the linearity of the Fourier Transform, it is possible to apply the DFT to each frame. The received signal can therefore be expressed as follows, where k denotes the Rx DFT output index:
$\forall k$

$$\begin{aligned} R(k) &= \sum_{t=0}^{N-1} \left(\sum_{m=0}^{KM-1} g(m) s(r_0,t) e^{j\frac{2\pi}{M}r_0 m} \right) e^{-j\frac{2\pi}{NM/2}(m+t\frac{M}{2})k} \\ &= s_{r_0} G\left(k - r_0\frac{M}{2}\right) \sum_{t=0}^{N-1} e^{j\frac{2\pi}{N}(q-k)t} \\ &= s_{r_0} G\left(k - r_0\frac{M}{2}\right) D(q-k) \end{aligned} \quad (4)$$

where $g(m)$ is the impulse response of the filter (of size KM), $G(x) = \sum_{m=0}^{KM-1} g(m) e^{-j\frac{2\pi}{MN/2}xm}$ is the frequency response of the filter g with a frequency resolution of $\frac{1}{MN/2}$ and $D(x) = \sum_{t=0}^{N-1} e^{j\frac{2\pi}{N}tx}$.

It can be easily proved by means of angle transformation formulae that the function $D(x)$ is N-periodic. Therefore, the function will be studied in the interval $I_x = [-\frac{N}{2}, \frac{N}{2}]$. We have the following results :
$\forall x \in I_x$

$$D(x) = \begin{cases} N \text{ for } x = 0 \\ 0 \text{ otherwise} \end{cases} \quad (5)$$

Regarding (5), the only possibility that only an unique value of k (in $I_k = [\lfloor -\frac{N}{2} - q \rfloor, \lfloor \frac{N}{2} - q \rfloor]$) receives the signal is that $(q-k) = 0$. In other words, this result states that, for a signal transmitted over a given sub-carrier q, the corresponding received signal is localized in an unique Rx DFT output index k among an interval of size N. Besides, if two signals are transmitted over two distinct IDFT sub-carriers $q_1 \neq q_2$, their corresponding received signal will be localized at two distinct Rx DFT output indexes without interfering one with the other. This situation will be studied in further detail in the next section.

The total number of DFT output indexes is $\frac{MN}{2}$. It is assumed for the rest of the paper that there is a fair distribution of the indexes among the M carriers of the system, i.e. there is a group of $\frac{N}{2}$ indexes dedicated per carrier. It is also assumed that the input signal's normalized bandwidth is $\frac{1}{2}$. It implies that the allocation of a carrier's indexes is contiguous.

Besides, the frequency response of the filter G is assumed to be centred on the considered carrier DFT index block. Let us denote the Rx DFT indexes related to carrier r_0 by k_{r_0}. By applying the aforementioned assumptions, we obtain:

$$-\frac{N}{4} \leq k_{r_0} - r_0\frac{M}{2} < \frac{N}{4} \quad (6)$$

A relation between the pulsation q of the input signal and the output indexes k_{r_0} can be derived from (5):

$$k_{r_0} = q + \alpha N \text{ where } N \in \mathbb{Z} \quad (7)$$

By inserting (7) in (6), it is possible to derive a condition on q given in (8).

$$\begin{cases} -N/4 \leq q \leq +N/4 - 1 \text{ if } r_0 \text{ is even} \\ N/4 \leq q \leq +3N/4 - 1 \text{ otherwise} \end{cases} \quad (8)$$

This is the intra-carrier orthogonality condition. It states that if the pulsation of the input signal satisfies (8), it will be received at an unique DFT output index inside the carrier's available indexes k_{r_0}.

D. Quasi-Orthogonality and Filter Pre-compensation

By considering the latter result and the linearity of the system, it is possible to feed several precoding DFT subcarrier up to $\frac{N}{2}$ and the sub-carrier indexes q must satisfy (8). The signal feeding the filter bank becomes:

$$s(r,t) = \begin{cases} \sum_{q\in\Omega_r} s_{r_0,q} e^{j\frac{2\pi}{N}q(t-N_{CP})} \text{ for } r = r_0 \\ 0 \text{ otherwise} \end{cases} \quad (9)$$

where Ω_r is the set of the $\frac{N}{2}$ possible values of q defined by (8).

Given the considered input signal, the received signal can be expressed as shown in (10).
$\forall\ k$,

$$\begin{aligned} R(k) &= \sum_{t=0}^{N-1} \sum_{m=0}^{KM-1} g(m) \left(\sum_{r=0}^{M-1} s(r,t) e^{j\frac{2\pi}{M}rm} \right) e^{-j\frac{2\pi}{MN/2}(m+t\frac{M}{2})k} \\ &= \sum_{t=0}^{N-1} G(k - r_0\frac{M}{2}) s(r_0,t) e^{j\frac{2\pi}{N}tk} \\ &= \sum_{t=0}^{N-1} G(k - r_0\frac{M}{2}) \left(\sum_{q\in\Omega_r} s_{r_0,q} e^{j\frac{2\pi}{N}qt} \right) e^{j\frac{2\pi}{N}tk} \\ &= G(k - r_0\frac{M}{2}) \sum_{q\in\Omega_r} s_{r,q} D(q-k) \end{aligned} \quad (10)$$

The power of the received signal for a configuration $(M,N) = (16,16)$ is depicted in Fig.3. We can observe that interference terms appear every two carrier indexes. This is induced by the N periodicity of the function D (as a reminder the size of a carrier block is $\frac{N}{2}$). However, the magnitude of the interference is managed by the filter frequency response that is added on the chart for illustration. For Fig.3, a Gaussian filter with Bandwidth-Time product of 0.28 is used.

This is the reason why the waveform is said to be quasi-orthogonal. Indeed, even if perfect intra-carrier orthogonality is ensured by conditions (2) and (8), interference is generated on other carriers, but nonetheless thanks to a good frequency

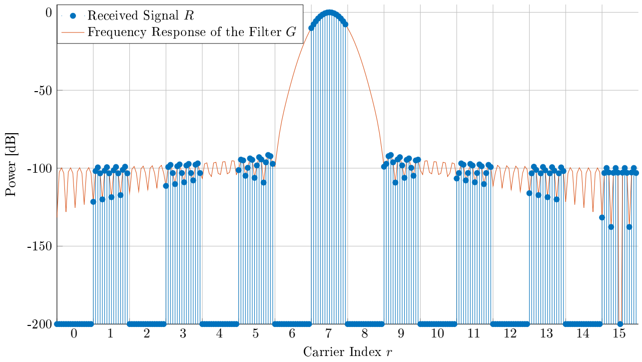

Figure 3. Transmission of a $\frac{N}{2}$-frequency-tone signal over carrier $r_0 = 7$

localization it is possible to bring the interference terms to an extreme low level so that the generated interference does not disturb transmission over the involved carriers. Explicit values of Signal-to-Interference Ratio (SIR) will be given later in the paper.

The transmitted signal is distorted by the filter response G as illustrated in Fig.3. The shape of the received signal is independent of the carrier index as it has been assumed that the frequency response is centred on the carrier block. This shaping of the signal implies that a filtering stage is necessary in reception in order to compensate it. Another solution is to use the linearity of the system and to compensate it at the transmitter side. The motivations to do so are multiple. First, we keep limiting the complexity of the receiver to a DFT. Then, the receiver does not need any knowledge of the filtering performed at the transmitter side (neither the filter shape nor the overlapping factor). It also prevents noise enhancement for highly attenuated carrier indexes.

A correspondence between the set of pulsations q and the sub-carriers indexes a is considered so that the sub-carrier index is always defined in $[0, \frac{N}{2} - 1]$:

$$a = \begin{cases} q + \frac{N}{4} & \text{if r is even} \\ q - \frac{N}{4} & \text{otherwise} \end{cases} \tag{11}$$

Considering (11), the filter pre-compensation can be expressed as follows, with x^* stands for the complex conjugate operator:

$$s_{r,a} = s'_{r,a} \frac{G^*(a - \frac{N}{4})}{|G(a - \frac{N}{4})|^2} \tag{12}$$

where $s'_{r,a}$ are complex symbols.
The expression of the received signal, with pre-compensation, can be expressed as follows with a the subcarrier index and r the carrier index.

$$\begin{aligned} R(a + r\frac{N}{2} - \frac{N}{4}) &= s_{r,a} \\ &+ \sum_{\substack{\epsilon \neq 0 \\ 0 \leq r+2\epsilon \leq M-1}} \frac{G^*(a - \frac{N}{4})G(a - \frac{N}{4} - \epsilon N)}{|G(a - \frac{N}{4})|^2} s_{r+2\epsilon,a} \end{aligned} \tag{13}$$

E. Final scheme

The block diagrams of the final scheme for the transmitter and the receiver are depicted in Fig.4 and Fig.5. One can observe that the receiver actually corresponds to a CP-OFDM receiver. The transmitter is composed of filter bank fed by M CP-OFDM modulators operating in parallel. A framing stage maps the $\frac{N}{2}$ OFDM sub-carriers according to the intra-carrier orthogonality condition (8). The additional pre-distortion stage compensates the filter distortion at the transmitter side.

It can be assumed that both N and M are power of two so the IDFTs in the transmitter can be implemented by means of IFFTs. It would imply that the DFT in reception can be implemented by means of FFT as well. The complexity of the transmitter will be assessed in the next section.

III. Key Performance Indicators

This section is dedicated to the KPIs assessment for the proposed waveform. A BF-OFDM configuration that gives an equivalent FFT size in reception to the legacy LTE CP-OFDM (i.e. 1024) will be considered: $(M, N, K) = (64, 32, 4)$. The CP is designed to satisfy the circularity condition (2) : $N_{\mathrm{CP}} = 7$.

A. Spectral Efficiency

Spectral efficiency (SE) is a key parameter for high data rate systems. The proposed scheme achieves a SE very similar to the legacy CP-OFDM. In both cases, there is a spectral loss induced by the insertion of a CP. Assuming, N_s the number of transmitted symbols, M_a the number of active filter bank carriers, η the modulation efficiency (including both the modulation order and the coding rate), the SE can be expressed as:

$$\begin{aligned} \eta_{\mathrm{BF-OFDM}} &= \frac{N_s M_a \frac{N}{2} \eta}{KM + \frac{M}{2}\left(N_s(N + N_{\mathrm{CP}}) - 1\right)} \\ &\xrightarrow{N_s \to \infty} \eta \frac{M_a}{M} \frac{N}{N + N_{\mathrm{CP}}} \end{aligned} \tag{14}$$

The spectral efficiency is reduced by the CP insertion as in CP-OFDM. Considering lower overlapping factor K (which relaxes the circularity condition and minimal CP size), is an efficient way to enhance the SE. In that case the level of interferences needs to be managed.

B. Complexity

Complexity evaluation is done by estimating the amount of complex multiply necessary to perform the transmitter function. Let N_{FFT} denotes the number of FFT size. Concerning OFDM, assuming a CooleyTukey FFT algorithm, the number of complex multiplication is equal to:

$$C^{\mathrm{OFDM}} = \frac{N_{\mathrm{FFT}}}{2} \log_2(N_{\mathrm{FFT}}) \tag{15}$$

The complexity of a BF-OFDM transmitter is the sum of the complexity of the pre-compensation stage, the M IFFT stages and the filter bank stage applied to $N + N_{\mathrm{CP}}$ set of samples. By considering that half of the inputs of the IFFT modulators are zeros and the sample repetition provided by the CP, we can express the complexity:

$$\begin{aligned} C^{\mathrm{BF-OFDM}} = \frac{MN}{2} &+ M\left(\frac{N}{2} + \frac{N}{2}\log_2\left(\frac{N}{2}\right)\right) \\ &+ N\frac{M}{2}\log_2(M) + KMN \end{aligned} \tag{16}$$

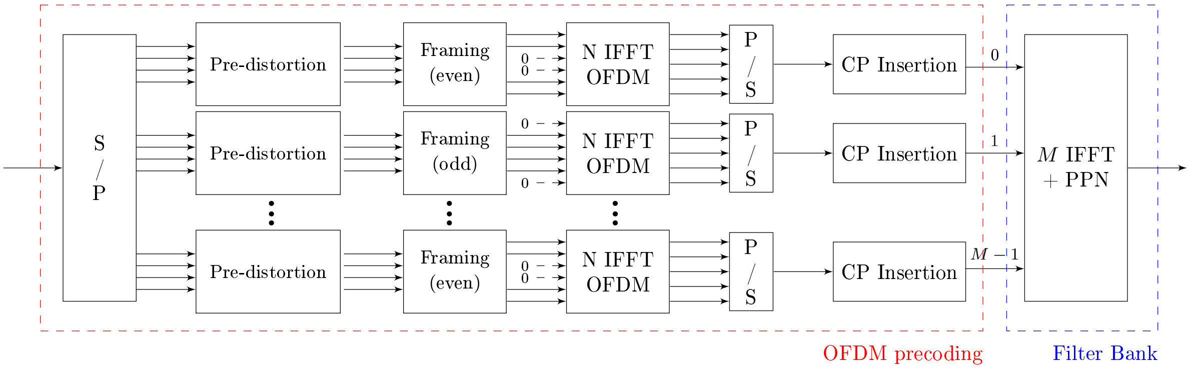

Figure 4. Transmitter scheme is based on a precoding and a filtering stages

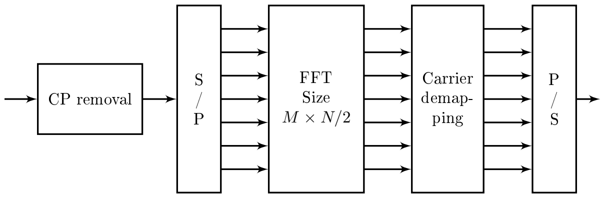

Figure 5. Receiver scheme corresponds to the one used in CP-OFDM

By considering a BF-OFDM configuration given earlier, the complexity ratio equals:

$$\frac{C^{\mathrm{BF-OFDM}}}{C^{\mathrm{OFDM}}} = 4.0 \tag{17}$$

The double-stage structure of the transmitter accounts for the complexity difference with CP-OFDM. However, the BF-OFDM transmitter provides an embedded sub-band filtering that is not the case of for CP-OFDM. Besides, additional complexity (with the pre-distortion) has been added in order to reduce the receiver to a FFT. The increase in complexity is thus justified and reasonable considering those two aspects.

C. Signal to Interference Ratio

The SIR is another key KPI as it is directly related to the quasi-orthogonality condition of the waveform. By assuming that the transmitted constellation is normalized to unity, the SIR can be expressed as follows, with $E[.]$ the expected value operator:

$$\mathrm{SIR} = \frac{P_{\mathrm{Sig}}}{P_{\mathrm{Int}}} = \frac{1}{\frac{1}{N/2}\sum_{a=0}^{N/2-1} E[P_{\mathrm{Int}}(a)]} \tag{18}$$

From (13) and by considering that the transmitted symbols are independent, one may find that:

$$\begin{aligned} E[P_{\mathrm{Int}}(a)] &= \left\| \sum_{\epsilon\neq 0} \frac{G^*(a-\frac{N}{4})G(a-\frac{N}{4}-\epsilon N)}{|G(a-\frac{N}{4})|^2} s_{r+2\epsilon,q} \right\|^2 \\ &= \sum_{\epsilon} \left\| \frac{G^*(a-\frac{N}{4})G(a-\frac{N}{4}-\epsilon N)}{|G(a-\frac{N}{4})|^2} \right\|^2 \end{aligned} \tag{19}$$

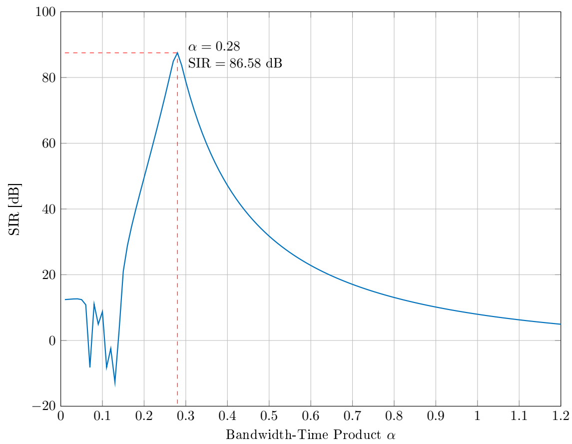

Figure 6. Optimization of the filter shape with respect to SIR criterion

It leads to

$$\mathrm{SIR} = \frac{1}{\frac{1}{N/2}\sum_{a=0}^{N/2-1}\left(\sum_{\epsilon\neq 0}\left\|\frac{G^*(a-\frac{N}{4})G(a-\frac{N}{4}-\epsilon N)}{|G(a-\frac{N}{4})|^2}\right\|^2\right)} \tag{20}$$

The SIR level is directly related to the frequency response of the filter. It is therefore possible to optimize a parameter-dependent filter w.r.t. to the SIR. For illustration, let us consider for instance the Gaussian filter with the Bandwidth-Time Product α as parameter. The optimization output is depicted in Fig.6.

We can observe that the parameter value highly impacts on the SIR and only a narrow interval of the parameter value leads to the highest SIR. $\alpha = 0.28$ gives the optimal SIR output.

The SIR has also been estimated for the PHYDYAS filter [10]. The results are given in Tab.I for $N = 32$.

BF-OFDM provides high SIR when combined with PHYDYAS filter shape and this value can even be increased

Table I. IMPACT OF THE FILTER SHAPE ON SIR, $K = 4$

Filter	PHYDYAS	Gaussian (BT=0.28)
SIR [dB]	61.02	86.58

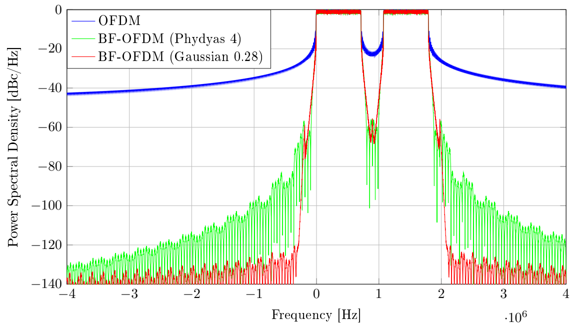

Figure 7. Power Spectral Density of CP-OFDM and BF-OFDM

by considering other filters as illustrated in Tab.I. These values justify the quasi-orthogonality property of the waveform. Indeed even if interference terms appear, the power ratio w.r.t. to the useful signal power is high enough not to affect high robustness against multipath channels and straightforward equalization and MIMO advanced techniques implementation like in CP-OFDM.

D. Power spectral density

The Power Spectral Density (PSD) of a waveform indicates how efficiently this waveform can use the spectrum bandwidth without interfering with systems using adjacent bands. An enhanced waveform is highly desirable for future wireless networks in order to benefit from spectrum sharing techniques.

The PSD of the BF-OFDM with both the PHYDYAS and Gaussian filters is depicted in Fig.7. The PSD of the legacy CP-OFDM is used as reference. One can observe that the BF-OFDM is better localized in the frequency domain thanks to its filtering stage. The Gaussian-shaped waveform provides sharper PSD decrease at the edges of the useful band, which is interesting for spectrum sharing techniques and multi-user scenarios.

Performance over frequency-selective channels and robustness to asynchronous adjacent transmissions are assessed by comparing BF-OFDM with other emerging modulation schemes in [15].

IV. Conclusion

In this paper, we have introduced a novel modulation scheme called BF-OFDM. We have described the transmitter and receiver scheme and derived constraints to maintain quasi orthogonality. We also give an analytical expression of the SIR that depends on the chosen filtering function. Thanks to this formulation, filters can be optimized to minimize SIR. We also assess some KPI such as, complexity, spectral efficiency as well as PSD.

The proposed waveform provides interesting assets for 5G applications: improved spectrum confinement, one-tap frequency domain equalization, high compatibility with MIMO techniques and resilience to ISI. Moreover, BF-OFDM also provides a high degree of flexibility and is specification transparent as it relies on a typical CP-OFDM receiver, which is innovative compared to the other 5G candidate waveforms.

This set of assets comes at the price of a transmitter slight complexity increase. However, it seems worth noticing that this complexity increase is nonetheless reasonable if future standardizations emphasize on such exhaustiveness for the air interface.

V. Acknowledgement

The authors would like to acknowledge the help of Rostom Zakaria for his wise advice.

This work has been performed in the framework of the WONG5 project, receiving funds from the French National Research Agency (ANR) under the contract number ANR-15-CE25-0005-02 as well as Horizon 2020 Project FANTASTIC-5G (ICT-671660) receiving funds from the European Union.

References

[1] N. G. M. N. Alliance, "5G White Paper," *online*, Feb. 2015.

[2] 5GPPP, "5G Archicture," *online*, 2016.

[3] R. H. Tehrani, S. Vahid, D. Triantafyllopoulou, H. Lee, and K. Moessner, "Licensed spectrum sharing schemes for mobile operators: A survey and outlook," *IEEE Communications Surveys Tutorials*, vol. PP, no. 99, p. 1, 2016.

[4] V. Vakilian, T. Wild, F. Schaich, S. ten Brink, and J. F. Frigon, "Universal-filtered multi-carrier technique for wireless systems beyond LTE," in *2013 IEEE Globecom Workshops (GC Wkshps)*, Dec 2013, pp. 223–228.

[5] J. B. Dore, R. Gerzaguet, and D. Ktenas, "5G Cellular Networks with Relaxed Synchronization: Waveform Comparison and New Results," in *2016 IEEE 83rd Vehicular Technology Conference (VTC Spring)*, May 2016, pp. 1–5.

[6] M. Matthe, D. Zhang, F. Schaich, T. Wild, R. Ahmed, and G. Fettweis, "A Reduced Complexity Time-Domain Transmitter for UF-OFDM," in *2016 IEEE 83rd Vehicular Technology Conference (VTC Spring)*, May 2016, pp. 1–5.

[7] M. Renfors, J. Yli-Kaakinen, and F. J. Harris, "Analysis and Design of Efficient and Flexible Fast-Convolution Based Multirate Filter Banks," *Proc. IEEE Transactions on Signal*, vol. 62, no. 15, pp. 3768–3783, Aug 2014.

[8] R. Chang, "High-speed multichannel data transmission with bandlimited orthogonal signals," *Bell Sys. Tech. J*, vol. 45, no. 10, pp. 1775–1796, 1966.

[9] H. G. Feichtinger and T. Strohmer, *Gabor analysis and algorithms : theory and applications*, ser. Applied and numerical harmonic analysis. Boston, Mass., Basel, Berlin: Birkhuser, 1998.

[10] M. Bellanger, "FBMC physical layer: a primer," ICT-PHYDYAS Project, Tech. Rep., 2010, available on http://www.ict-phydyas.org.

[11] R. Zakaria, "Transmitter and receiver design for inherent interference cancellation in MIMO filter-bank based multicarrier systems," Theses, Conservatoire national des arts et metiers - CNAM, Nov. 2012.

[12] R. Zakaria and D. L. Ruyet, "A novel FBMC scheme for Spatial Multiplexing with Maximum Likelihood detection," in *Wireless Communication Systems (ISWCS), 2010 7th International Symposium on*, Sept 2010, pp. 461–465.

[13] C. Lélé, P. Siohan, and R. Legouable, "The alamouti scheme with CDMA-OFDM/OQAM," *EURASIP J. Adv. Signal Process*, vol. 2010, pp. 2:1–2:11, Jan. 2010.

[14] J. Li, E. Bala, and R. Yang, "Ressource Block Filtered-OFDM for future spectrally agile and power efficient systems," *ELSEVIER Physical Communication*, vol. 11, pp. 36–55, June 2014.

[15] R. Gerzaguet, D. Demmer, J.-B. Doré, and D. Kténas, "Block-Filtered OFDM: a new promising waveform for multi-service scenarios," in *Proc. IEEE ICC 2017 Wireless Communications Symposium (ICC'17 WCS)*, Paris, France, May 2017.

[16] R. Zakaria and D. L. Ruyet, "A Novel Filter-Bank Multicarrier Scheme to Mitigate the Intrinsic Interference: Application to MIMO Systems," *IEEE Transactions on Wireless Communications*, vol. 11, no. 3, pp. 1112–1123, March 2012.

Block-Filtered OFDM: A new Promising Waveform for Multi-service Scenarios

Robin GERZAGUET*, David DEMMER*†, Jean-Baptiste DORÉ* and Dimitri KTÉNAS*
*CEA-Leti, Minatec Campus, Grenoble, France
{robin.gerzaguet, david.demmer, jean-baptiste.dore, dimitri.ktenas}@cea.fr
†Conservatoire National des Arts et Métiers, 292 Rue Saint-Martin, 75003 Paris, France.

***Abstract*—5G will have to cope with a high degree of heterogeneity in terms of services and requirements. Among these latter, flexible and efficient use of all available non-contiguous spectrums for different network deployment scenarios is one challenge for the future 5G. To maximize spectrum efficiency, the 5G air interface technology will also need to be flexible and capable of mapping various services to the best suitable combinations of frequency and radio resources. Such requirements are not satisfied by legacy CP-OFDM and alternative multicarrier waveforms such as UFMC and FBMC partially meet them. In this article, we introduce a new quasi-orthogonal waveform called Block-Filtered OFDM (BF-OFDM) that combines most of the advantages of the aforementioned waveforms at the price of slight complexity increase. Spectral localization and performance in multi-user scenario will be enhanced w.r.t OFDM and simple equalization as well as all classical MIMO schemes can be straightforwardly considered. The proposed waveform offers the same performance in presence of multipath channel as CP-OFDM and is also scalable which paves the way for future multi-service scenarios.**

I. Introduction

The fourth generation of wireless network (4G) is currently massively rolled-out but it is also known that it will quickly reach its limits. To face this issue, 3GPPP started to discuss 5G requirement during the RAN 5G workshop held in September 2015 leading to an emerging consensus that there will be a new, non-backward compatible, radio access technology as part of 5G [1].

As the availability of large amount of contiguous spectrum is getting more and more difficult to guarantee, the aggregation of non-contiguous frequency bands is considered for future generations of wireless networks (a.k.a. 5G) to meet higher data rates and/or improve access flexibility [2]. This requirement of spectrum agility has encouraged the study for alternative multicarrier waveforms to provide better adjacent channel leakage performance without compromising spectral efficiency (SE).

Even though Cyclic Prefix Orthogonal Frequency Division Multiplexing (CP-OFDM) is the most prominent multi-carrier modulation technique in wireless standards for below 6GHz transmission, it also exhibits some intrinsic drawbacks. An important frequency leakage is caused by its rectangular pulse shape and fine time and frequency synchronization is required to preserve the subcarrier orthogonality that guarantees a low level of intra and inter-cell interferences.

As a consequence several candidates have been extensively studied in the past few years among them Universal Filtered Multicarrier (UFMC also called UF-OFDM) [3], and Filter Bank Multicarrier (FBMC) combined with the use of Offset Quadrature Amplitude Modulation (OQAM) [4].

UFMC is a derivative of OFDM where a group of subcarriers is filtered in the frequency domain. It has been introduced by Alcatel-Lucent [3]. The subband filtering has been motivated by the fact that the smallest allocation resource in 3GPP-LTE is a resource block (RB), which is a group of twelve subcarriers. It leads to a better spectrum confinement, parametrized by the prototype filter. UFMC also outperforms OFDM in multi-user asynchronous scenario, due to its better spectral localization [5]. However, as the CP is replaced by a soft symbol transition due to the additional filtering operation, resistance against high frequency selective channel is low compared to CP-OFDM. The complexity increase compared to OFDM is in the order of 10 at the transmitter and 2 on the receiver for a full uplink LTE allocation and can be reduced at a price of a small performance decrease [6].

FBMC waveforms are subcarrier-wise filtering waveforms, as each subcarrier is filtered by a time-frequency translated prototype filter. The localization in both the time and frequency domains is managed by the choice of the prototype filters leading to lower Out of Band (OOB) radiations compared to OFDM. FBMC-OQAM can asymptotically achieve maximal SE due to the absence of CP. As the users are perfectly localized in the frequency domain, it also offers the best performance among the latter waveforms in multi-user asynchronous access when a guard subcarrier is introduced [5], [7]. The main drawbacks of FBMC are i) the long pulse shape impulse response that is not suitable for short bursts transmission ii) scattered pilot insertion iii) and MIMO support due to the use of OQAM (real orthogonality). It is clear that there is some place left to build an effective waveform that addresses most of the weakness of the aforementioned candidates. The aim of the paper is to propose a new quasi-orthogonal waveform that offers a better spectral localization than OFDM and a similar performance against frequency selective channels. Good performance in multiuser asynchronous scenarios are also of paramount importance. The compatibility of the proposed waveform with MIMO techniques and channel equalization should be straightforward. The waveform should be scalable and should cope with the expected various scenarios future wireless standards will face. In this paper, we introduce the Block Filtered OFDM (BF-OFDM) as a new promising quasi-orthogonal waveform.

The transmitter consists in concatenating M OFDM stages and a filterbank. Additional pre-processing in the transmitter is done in order to have a simple receiver scheme based on a FFT, followed by a one tap equalization. This scheme offers better spectral localization, better performance in multi-user scenario. Performance of the proposed waveform is assessed in terms of Power Spectral Density (PSD), SE, multipath channel resistance and multi-user asynchronous scenario. The associated mathematical framework and theoretical analysis of BF-OFDM is derived in [8].

This paper is organized as follows: a brief recall of legacy CP-OFDM and FBMC-OQAM are done in Section II. BF-OFDM description is proposed in Section III. A complexity analysis is proposed in section IV. The simulated results for power spectral density, multipath channel resistance and multi-user access scheme scenario are assessed in Section V. Eventually the last section draws some conclusions.

II. CP-OFDM AND FBMC RECALL

In this section, we propose to briefly recall the main characteristics of CP-OFDM and FBMC-OQAM. Indeed, the proposed waveform combines many aspects of these waveforms, such as IFFT/FFT stages, filter bank stage and CP insertion.

A. CP-OFDM

The OFDM transceiver scheme is depicted in Figure 1. The important characteristic of OFDM is that the frequency to time (resp. time to frequency) transform can be done with an Inverse Fast Fourier Transform (IFFT) (resp. FFT) process of size N and thus allows a low complexity transceiver. Besides, as the total bandwidth is divided into N subcarriers, the channel equalization can be reduced as a one tap coefficient per subcarrier if the coherence bandwidth of the channel is large enough. Finally, as the subcarrier orthogonality can be broken by the channel effect (leading to strong inter-carrier interference), a cyclic prefix (CP) is inserted, i.e. the end of the symbol is appended to its beginning. The CP guarantees circularity of the OFDM symbol (and thus no inter-carrier interference) if the delay spread of the channel is lower than the CP length.

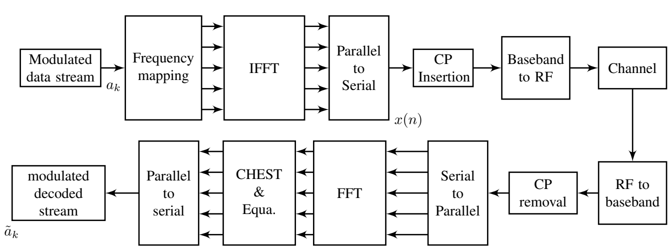

Fig. 1. CP-OFDM transceiver scheme

B. FBMC-OQAM

In FBMC, a set of parallel data symbols are transmitted with the use of modulated filters. The choice of the prototype filter controls the localization in frequency of the generated pulse and can provide better adjacent channel leakage performance in comparison to OFDM. OQAM combined with Nyquist constraints on the prototype filter is used to guarantee orthogonality (in the real field) between adjacent symbols and adjacent carriers while providing maximum SE. The duration L of the prototype filter is a multiple of the size of the FFT, N, so that $L = KN$, K is an integer and usually referred as to the overlapping factor.
The FBMC transmitter-receiver structure is depicted in Figure 2. It can be efficiently implemented using IFFTs or FFTs combined with a PolyPhase Network (PPN) [9]. QAM symbols are converted into OQAM symbol and then feed to a N IFFT. Then, pulse shaping is applied with the use of a PPN. To maximize the SE symbols overlap in time domain. Each symbol lasts KN and successive symbols are spaced by $N/2$ samples.

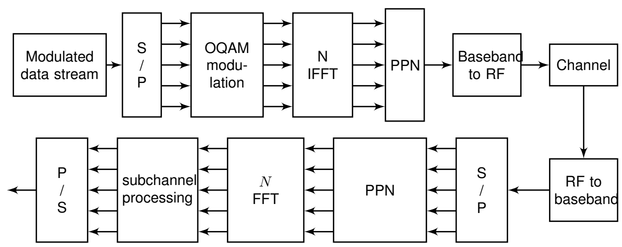

Fig. 2. FBMC-OQAM transceiver scheme (with PPN scheme)

C. Discussion and motivation

As stated in the introduction, these two waveforms exhibits strong advantages and strong drawbacks. For OFDM, simple implementation, simple equalization, straightforward MIMO application are counterbalanced by its poor spectral localization, and low performance in multi-user scenario. For FBMC-OQAM, its suitability in multi-user scenario is a strong advantage, but its low compatibility with OFDM (scattered pilot insertion, MIMO, . . .) makes the waveform difficult to adapt.
According to [10] the new air interface targets a single technical framework addressing all usage scenarios, requirements and deployment scenarios defined in TR38.913 [11] including enhanced mobile broadband (eMBB), massive machine-type-communications (mMTC) and ultra-reliable and low latency communications (URLLC). Additional support for very high velocities is also foreseen. These diverse services motivate a highly flexible waveform allowing very different configurations. On the one hand, long symbol durations and thus smaller subcarrier spacings are attractive for high delay spreads and multicast/broadcast services. On the other hand, short symbol durations and thus larger subcarrier spacings are desirable for low latency and high velocity use cases. The answer of LTE design to these issues was a compromise numerology that traded off the objectives of all purposes. This compromise has its limitations with respect to supporting newer traffic requirements, such as high velocities and low latencies.

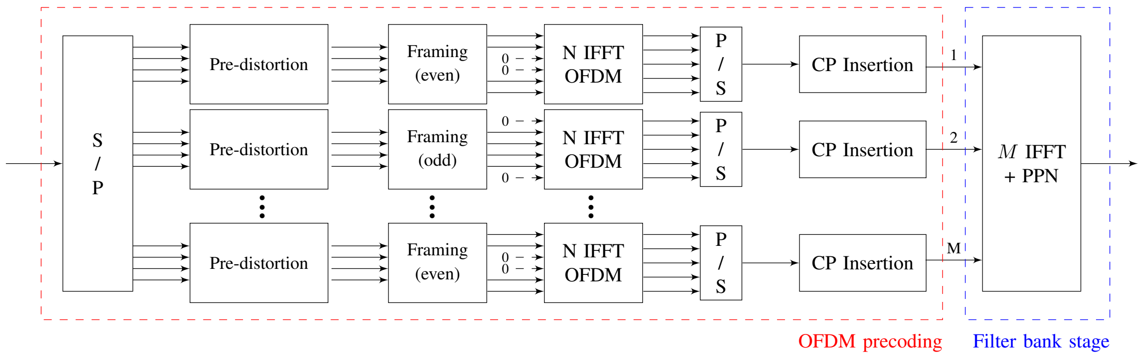

Fig. 3. BF-OFDM transmitter scheme

Furthermore, small sporadic packets sent in mMTC traffic requires relaxing synchronicity in order to reduce the protocol overhead. Last but not least, according to the agreement of 3GPP RAN1-86 meeting held in August 2016, new waveforms for the phase 1 of 5G (New Radio Work Item) should be specification transparent, i.e. the receiver does not need to know the filtering/windowing used at transmitter.
The proposed waveform will combine most of the advantages of the aforementioned waveform at the price of slightly complexity increase on the transmitter side while keeping a simple OFDM receiver. Spectral localization and performance in multi-user scenario will be enhanced w.r.t OFDM while keeping a simple OFDM receiver. Contrary to UFMC, the CP ensures circularity of the signal and thus offers the same performance in presence of multipath channel as legacy CP-OFDM. The proposed solution is also scalable which paves the way for future multi-service scenarios.

III. BF-OFDM PROPOSAL

In this section, we describe the new waveform scheme with the transmitter and receiver architectures.

A. Transmitter scheme

The transmitter scheme is depicted in Figure 3. We denote M the number of carriers, and N the number of subcarriers. There are N subcarriers per carrier. To maintain orthogonality, only $N/2$ subcarriers bear data per carrier. The subcarrier allocation depends on the carrier index parity.
For each BF-OFDM symbol, $N/2$ data are mapped in frequency domain, an IFFT of size N is applied to each carrier, and a CP is appended. It ensures the circularity of the received signal. The output of the M stages are then fed to a filter bank parametrized by a prototype filter with an overlapping factor K. As in typical FBMC transmitter, an overlap and sum operation is realized by the PPN. Symbols are then transmitted each $M/2$ samples.
A predistortion stage is applied to each subcarrier, and has two objectives: i) ensures that the receiver stage can be based on single FFT ii) compensates the effect of the distortion of the filter bank (phase and amplitude). The insertion of a CP aims to avoid inter-symbol interference (ISI) and makes simple the equalization in the frequency domain. In the case of BF-OFDM waveform, ISI is the result of the convolution of the multipath channel and the prototype filter. Therefore, a direct link between the minimal size of the CP and the overlapping factor exists and is expressed as $N_{\text{CP}} \geq 2K-1$. It should be noted that in practice the size of the CP can be reduced at the price of a negligible interference level.
In terms of complexity, one can see a slightly increase compared to OFDM. A complexity analysis is assessed in Section IV.

B. Receiver scheme

The receiver scheme is depicted in Figure 4. It consists on selecting a window of size $MN/2$ each $N_{CP}M/2 + MN/2$ samples. It is followed by a $MN/2$ FFT stage. The receiver is thus with low complexity, similar to the one of CP-OFDM.

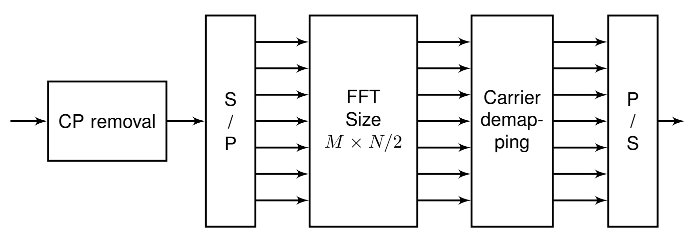

Fig. 4. BF-OFDM receiver scheme

IV. COMPLEXITY

Complexity evaluation is done by estimating the amount of complex multiply necessary to perform the transmitter function. Concerning OFDM, assuming a Cooley-Tukey FFT algorithm, the number of complex multiplications is equal to:

$$C^{\text{OFDM}} = \frac{N_{\text{FFT}}}{2} \log_2 (N_{\text{FFT}}) + C_f^{\text{OFDM}} \tag{1}$$

where C_f^{OFDM} is the complexity associated with the filtering function applied to an OFDM signal. The complexity of a BF-OFDM transmitter is the sum of the complexity of the pre-compensation stage, the M_a OFDM stages (M_a is the number of active carriers) and the filter bank stage applied

TABLE I
COMPLEXITY EVALUATION NORMALIZED TO THE COMPLEXITY OF THE RECEIVED FFT WHEN $K = 4$ AND $N_{CP} = 4$

M / N	16	32	64	128	256
16	4.14	3.75	3.44	3.20	3.00
32	3.88	3.56	3.30	3.09	2.92
64	3.67	3.40	3.18	3.00	2.85
128	3.50	3.27	3.08	2.92	2.79
256	3.36	3.17	3.00	2.86	2.73

to $N + N_{\mathrm{CP}}$ set of samples where N_{CP} is the CP length. Using the properties that $N/2$ samples are zeros at the input of the OFDM stage, the complexity is reduced to:

$$C^{BF-OFDM} = \frac{M_a N}{2} + M_a \left(\frac{N}{2} + \frac{N}{2}\log_2\left(\frac{N}{2}\right)\right) + \frac{NM}{2}\log_2(M) + KMN \tag{2}$$

An evaluation of the complexity is done using typical parameter of M and N assuming that half of the carriers are active. Results are provided in Table I. The complexity is normalized to the complexity of the received FFT. We assume $K = 4$ and $N_{CP} = 4$. For a typical scenario where $N = 64$ and $M = 128$, the transmitter is 3 times more complex than the received FFT. This complexity increase is reasonable and makes sense if the frequency localization of the waveform is of interest. Indeed, with our proposed waveform, the filtering operation is embedded contrary to classic OFDM where additional filter stages can dramatically increase the overall complexity. The complexity enhancement is also limited compared to UFMC [6] thanks to the embedded filter bank. The complexity increase of UFMC compared to OFDM is in the order of 10 at the transmitter and 2 on the receiver for a full uplink LTE allocation and can be reduced at a price of a small performance decrease [6].

V. PERFORMANCE EVALUATION

In this section we compare the performance of the proposed BF-OFDM scheme and OFDM, UFMC and FBMC. SE, PSD, performance over multipath channel and robustness to non-synchronous adjacent transmission are assessed.

A. BF-OFDM parametrization

CP-OFDM is parametrized by the FFT size, the subcarrier spacing, the CP size and the number of allocated carriers. BF-OFDM is parametrized by the filter bank FFT size, the carrier bandwidth, the OFDM precoding FFT size and the CP size. The proposed waveform is scalable, and different configurations can be used to optimize the performance w.r.t a given indicator. For a given carrier number M, better frequency resolution can be obtained by increasing the number of subcarrier per carrier. On the contrary, one can imagine to decrease the number of subcarrier per carrier or increase the carrier bandwidth to reduce the Rx FFT size in order to allow better resistance in high mobility scenarios. Prototype filter can also be optimized to fulfill a target requirement.
Finally, it should be noted that that compatibility with legacy

TABLE II
SIMULATION PARAMETERS

OFDM parameters	
FFT size	1024
CP length	72
Number of Resource blocks	50
Number of active subcarriers	$50 \times 12 = 600$
Sampling Frequency F_e	15.36 MHz (15kHz subcarrier spacing)
RB bandwidth	180 kHz
UFMC parameters	
FFT size, F_e, subcarrier spacing	same as OFDM
Filter	Dolph-Chebyshev, 73 taps, 40dB rejection
FBMC parameters	
FFT size, F_e, subcarrier spacing	same as OFDM
Filter	Phydyas, $K = 4$
BF-OFDM parameters	
M	128
N	64
Rx FFT size	4096
CP size	4
Number of active carriers	50
Number of active subcarriers	$50 \times 32 = 1600$
Carrier bandwidth	180 kHz
Sampling Frequency	23.04 MHz
Prototype Filter	Phydyas, $K = 4$

CP-OFDM can also be obtained. A possible way to achieve this is to set a carrier bandwidth equal to an OFDM resource block (*i.e.* 180kHz). In this paper we propose to use 32 data-bearing subcarrier per carrier as it is a suitable trade-off between the different evaluation criteria. We will consider the parameters described in Table II. We will focus on OFDM, UFMC (following a classic parametrization [12]) FBMC, and BF-OFDM.

B. Spectral efficiency

To unleash very high data rates, spectral efficiency, is a matter of importance. The proposed scheme offers similar SE compared to OFDM. There is in both case a spectral loss due to the cyclic prefix insertion.
For OFDM, assuming a FFT of size N_{FFT} a CP of size N_{C} and N_{a} active carriers, and denoting η the modulation efficiency (including modulation order and coding rate), the SE can be expressed as:

$$\eta_{\mathrm{OFDM}} = \frac{N_{\mathrm{a}}\eta}{N_{\mathrm{C}} + N_{\mathrm{FFT}}}$$

UFMC SE is the same as the one of OFDM, as the filter length is set to $L = N_C + 1$ and same subcarrier allocation is done. For FBMC, the SE depends on the number of transmitted symbols, denoted N_s and is expressed as:

$$\eta_{\mathrm{FBMC}} = \frac{N_{\mathrm{a}} \times \eta \times N_s}{(2N_s - 1)\frac{N_{FFT}}{2} + KN_{FFT}} \xrightarrow{N_s \to \infty} \frac{N_{\mathrm{a}} \times \eta}{N_{FFT}}$$

Similarly for BF-OFDM, we assume M carriers with M_{a} active carriers; each of them with a N FFT size for the precoding stage. With the same aforementioned modulation efficiency η and number of transmitted symbols N_s, the SE is expressed as:

$$\eta_{\mathrm{BF-OFDM}} = \frac{N_s \times M_{\mathrm{a}}\frac{N}{2}\eta}{[N_s(N + N_{\mathrm{CP}}) - 1]\frac{M}{2} + KM} \xrightarrow{N_s \to \infty} \frac{M_{\mathrm{a}}}{M} \times \frac{N \times \eta}{N + N_{\mathrm{CP}}} \tag{3}$$

In (3), $M_{\mathrm{a}}N/2$ stands for the number of active subcarriers (equivalent to the N_{a} for OFDM). (V-B) and (3) means that similar spectral efficiency can be obtained if the BF-OFDM CP overhead ($M \times N_{CP}$ / $(M \times N)$) is similar to the one of OFDM (N_c/N_{FFT}).
On Figure 5, we compare the throughput ratio between several waveform and OFDM, w.r.t to a given slot duration with $\eta = 1$ and using parameters defined in Table II. If the duration of the slot increases, best SE is obtained with FBMC as there is no SE loss due to CP insertion. OFDM and BF-OFDM SE offers similar performance as the CP overhead is the same. For short bursts, one can find a configuration where BF-OFDM offers a slightly better throughput compared to OFDM. It is also shown that for short bursts, throughput for BF-OFDM is better when compared to FBMC-OQAM.

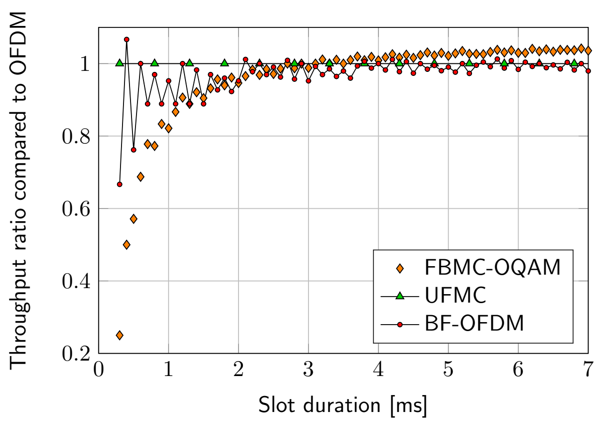

Fig. 5. Spectral efficiency comparison

C. Power spectral density

We now compare the power spectral density of the proposed waveform. We allocate the same bandwidth for all waveforms. It should be noted that in the proposed configuration, an OFDM RB is equivalent to a BF-OFDM carrier. We have allocated 2 groups of 4 RBs separated by 2 RBs. PSD of OFDM, UFMC, FBMC and BF-OFDM are depicted in Figure 6. We show that best spectral localization is obtained with FBMC, as this waveform has been optimized for low OOB leakage at the price of real orthogonality. BF-OFDM is better localized in frequency domain compared to OFDM and UFMC. In addition to very low OOB leakage at the edge of the band, we also show that the power spectral density between two adjacent bands decreases rapidly for BF-OFDM, which is interesting for spectrum sharing perspectives.

D. Performance against multipath channel

As the proposed waveform has the same receiver structure as OFDM, performance with multipath channel are very similar. In the proposed configuration, the BF-OFDM frequency resolution is slightly higher (5.625 kHz for BF-OFDM vs 15 kHz for OFDM). We depict in Figure 7 the performance of OFDM, UFMC, FBMC and the proposed BF-OFDM in presence of a Type Delay Line -C (TDL-C) channel model scaled with

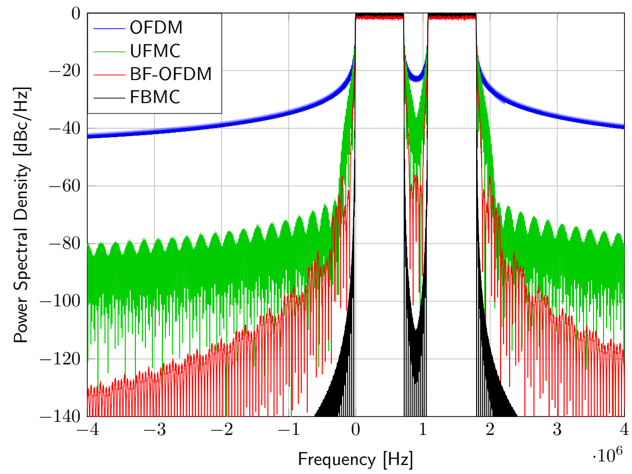

Fig. 6. Power spectral density of OFDM and BF-OFDM

a delay spread of $1\mu s$ [13]. We compute the Block Error Rate with a Turbo Decoder with 8 iterations, and segments of size 6144 bits, assuming 64-QAM of rate 1/2. The proposed waveform has similar performance compared to OFDM, and outperforms UFMC that suffers from ISI.

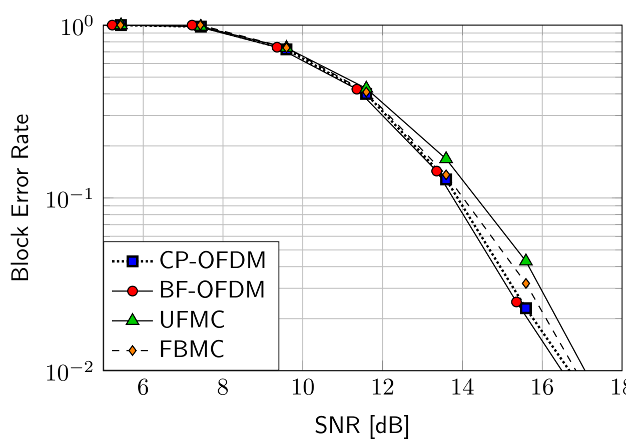

Fig. 7. Performance with TDL-C channel model (delay spread parameter of $1\mu s$)

E. Performance in multi-user asynchronous scenario

We finally assess the performance in a typical multi-user asynchronous scenario as it is currently discussed in standardization [14]. We consider two users, one (UE0 with 3 allocated RBs) synchronized with its serving base station, and another one (UE1 with 9 allocated RBs) that is unsynchronized with UE0 and the BS. UE0 et UE1 share the same numerology parameters (See Table II). We consider the performance of UE0 after equalization. Due to delay and frequency errors, UE1 will interfere with UE0 and the performance degradation depends on the chosen waveform [5].
In Figure 8, we represent the Mean Square Error (MSE) obtained for different guard bands and CFO, and different delays for OFDM, UFMC, FBMC and BF-OFDM. For UFMC,

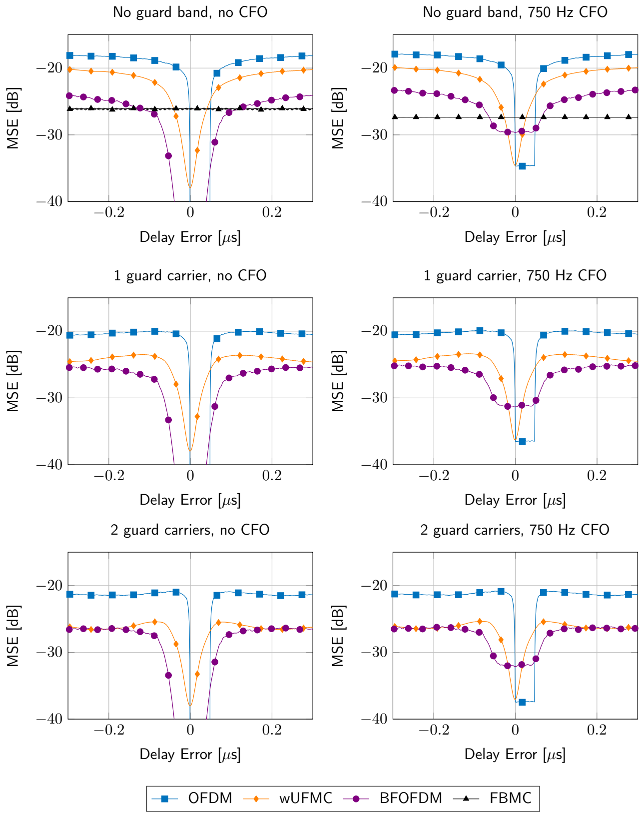

Fig. 8. Performance in multi-user asynchronous scenario

an additional windowing has been set on the receiver side to improve the performance [2], [5], [7]. If a guard carrier is inserted, best performance is obtained with FBMC (performance are below the lower limit of -40 dB). This is done at the price of complex orthogonality which rises several strong drawbacks ((MIMO compatibility, scattered pilot insertion, ...) as already stated. BF-OFDM offers very good performance, and greatly outperforms OFDM and UFMC. If no guard carrier is inserted (contiguous allocation), the proposed waveform outperforms OFDM (out of CP range),UFMC and FBMC (same performance is observed for very large delay errors). Impact of CFO is comparable for all waveforms and tend to limit the overall performance. The proposed solution is promising in multi-user asynchronous scenario as it offers very good performance (especially for low delay errors) while keeping advantages of orthogonal waveforms.

VI. Conclusions

Flexible and efficient use of non-contiguous unused spectrum targeting heterogeneous mobile network deployment scenarios is one of the key challenges that future 5G systems would need to tackle. In this paper we have presented a new promising waveform called Block-Filtered OFDM that addresses most of the weakness of legacy OFDM in terms of spectral localization and performance in asynchronous scenario, while keeping complex quasi orthogonality and simple FFT based receiver. Performance in several representative criteria have been assessed (spectral efficiency, power spectral density, performance against multipath channel and performance in multi-user asynchronous scenario). We have compared the performance of BF-OFDM OFDM, UFMC and FBMC-OQAM regarding these criteria, showing the potential benefits of the proposed scheme. Besides, a complexity analysis has been provided, showing that the scalability and flexibility of BF-OFDM can be done as a price a slightly complexity increase.

VII. Acknowledgement

This work has been performed in the framework of the Horizon 2020 project FANTASTIC-5G (ICT-671660) receiving funds from the European Union. The authors would like to acknowledge the contributions of their colleagues in the project, although the views expressed in this contribution are those of the author and do not necessarily represent the project.

References

[1] G.-R. G. Workshop, September 2015. [Online]. Available: http://www.3gpp.org/news-events/3gpp-news/1734-ran_5g.
[2] G. Wunder, P. Jung, M. Kasparick, T. Wild, F. Schaich, Y. Chen, S. Brink, I. Gaspar, N. Michailow, A. Festag, L. Mendes, N. Cassiau, D. Ktenas, M. Dryjanski, S. Pietrzyk, B. Eged, P. Vago, and F. Wiedmann, "5GNOW: non-orthogonal, asynchronous waveforms for future mobile applications," *Communications Magazine, IEEE*, vol. 52, no. 2, pp. 97–105, February 2014.
[3] V. Vakilian, T. Wild, F. Schaich, S. ten Brink, and J.-F. Frigon, "Universal-filtered multi-carrier technique for wireless systems beyond LTE," in *Proc. IEEE Globecom Workshops (GC Wkshps)*, Dec 2013, pp. 223–228.
[4] J.-B. Dore, V. Berg, and D. Ktenas, "Channel estimation techniques for 5G cellular networks: FBMC and multiuser asynchronous fragmented spectrum scenario," *Transactions on Emerging Telecommunications Technologies*, vol. 26, no. 1, pp. 15–30, 2015.
[5] J.-B. Dore, R. Gerzaguet, and D. Ktenas, "5G Cellular Networks with Relaxed Synchronization: Waveform Comparison and New Results," in *Proc. VTC Spring Workshop on 5G air interface*, 2016.
[6] M. Matthe, D. Zhang, F. Schaich, T. Wild, R. Ahmed, and G. Fettweis, "A reduced complexity time-domain transmitter for UF-OFDM," in *Proc. IEEE 83rd Vehicular Technology Conference (VTC)*, May 2016, pp. 1–5.
[7] R. Gerzaguet, N. Bartzoudis, L. G. Baltar, V. Berg, J.-B. Doré, D. Kténas, O. Font-Bach, X. Mestre, M. Payaró, M. Färber, and K. Roth, "The 5g candidate waveform race: a comparison of complexity and performance," *EURASIP Journal on Wireless Communications and Networking*, vol. 2017, no. 1, p. 13, 2017. [Online]. Available: http://dx.doi.org/10.1186/s13638-016-0792-0
[8] D. Demmer, R. Gerzaguet, J.-B. Doré, D. Le Ruyet, and D. Kténas, "Block-Filtered OFDM: an exhaustive waveform to overcome the stakes of future wireless technologies," in *Proc. IEEE ICC 2017 Wireless Communications Symposium (ICC'17 WCS)*, Paris, France, May 2017.
[9] P. Siohan, C. Siclet, and N. Lacaille, "Analysis and design of OFDM/OQAM systems based on filterbank theory," *IEEE Transactions on Signal Processing*, vol. 50, no. 5, pp. 1170–1183, May 2002.
[10] RP-160671, "New sid proposal: Study on new radio access technology," March 2016.
[11] TR38.913, "Study on scenarios and requirements for next generation access technologies," October 2016.
[12] X. Wang, T. Wild, and F. Schaich, "Filter optimization for carrier-frequency- and timing-offset in universal filtered multi-carrier systems," in *Proc. IEEE 81st Vehicular Technology Conference (VTC Spring)*, May 2015, pp. 1–6.
[13] 3GPP TR 38.900, "3rd Generation Partnership Project; Technical Specification Group Radio Access Network; Channel model for frequency spectrum above 6 GHz (Release 14)," 2016.
[14] "3GPP TSG RAN WG1, R1-163558, way forward on assumptions for waveform evaluation," April 2016.